

Approximate constructions of counterdiabatic driving with NMR quantum systems

Hui Zhou(周辉), Xiaoli Dai(代晓莉), Jianpei Geng(耿建培), Yunlan Ji(季云兰), and Xinhua Peng(彭新华)

Citation: Chin. Phys. B, 2024, 33 (**9**): 090301. DOI: 10.1088/1674-1056/ad58b2
Journal homepage: http://cpb.iphy.ac.cn; http://iopscience.iop.org/cpb

What follows is a list of articles you may be interested in

Variational quantum simulation of the quantum critical regime

Zhi-Quan Shi(石志全), Xu-Dan Xie(谢旭丹), and Dan-Bo Zhang(张旦波)
Chin. Phys. B, 2023, 32 (**8**): 080305. DOI: 10.1088/1674-1056/accb43

Variational quantum simulation of thermal statistical states on a superconducting quantum processer

Xue-Yi Guo(郭学仪), Shang-Shu Li(李尚书), Xiao Xiao(效骁), Zhong-Cheng Xiang(相忠诚), Zi-Yong Ge(葛自勇), He-Kang Li(李贺康), Peng-Tao Song(宋鹏涛), Yi Peng(彭益), Zhan Wang(王战), Kai Xu(许凯), Pan Zhang(张潘), Lei Wang(王磊), Dong-Ning Zheng(郑东宁), and Heng Fan(范桁)
Chin. Phys. B, 2023, 32 (**1**): 010307. DOI: 10.1088/1674-1056/aca7f3

Quantum simulation of lattice gauge theories on superconducting circuits: Quantum phase transition and quench dynamics

Zi-Yong Ge(葛自勇), Rui-Zhen Huang(黄瑞珍), Zi-Yang Meng(孟子杨), and Heng Fan(范桁)
Chin. Phys. B, 2022, 31 (**2**): 020304. DOI: 10.1088/1674-1056/ac380e

Nuclear magnetic resonance for quantum computing: Techniques and recent achievements

Tao Xin(辛涛), Bi-Xue Wang(王碧雪), Ke-Ren Li(李可仁), Xiang-Yu Kong(孔祥宇), Shi-Jie Wei(魏世杰), Tao Wang(王涛), Dong Ruan(阮东), Gui-Lu Long(龙桂鲁)
Chin. Phys. B, 2018, 27 (**2**): 020308. DOI: 10.1088/1674-1056/27/2/020308

Robustness of quantum discord to sudden death in nuclear magnetic resonance

Xu Jian-Wei(胥建卫) and Chen Qi-Hui(陈起辉)
Chin. Phys. B, 2012, 21 (**4**): 040302. DOI: 10.1088/1674-1056/21/4/040302

TOPICAL REVIEW — Quantum computing and quantum sensing

Approximate constructions of counterdiabatic driving with NMR quantum systems

Hui Zhou(周辉)[1,†], Xiaoli Dai(代晓莉)[1], Jianpei Geng(耿建培)[1], Yunlan Ji(季云兰)[1], and Xinhua Peng(彭新华)[2,3,4,‡]

[1] *School of Physics, Hefei University of Technology, Hefei* 230009, *China*
[2] *Chinese Academy of Sciences Key Laboratory of Microscale Magnetic Resonance and School of Physical Sciences, University of Science and Technology of China, Hefei* 230026, *China*
[3] *Chinese Academy of Sciences Center for Excellence in Quantum Information and Quantum Physics, University of Science and Technology of China, Hefei* 230026, *China*
[4] *Hefei National Laboratory, University of Science and Technology of China, Hefei* 230088, *China*

(Received 30 April 2024; revised manuscript received 13 June 2024; accepted manuscript online 15 June 2024)

Counterdiabatic driving (CD) offers a fast and robust route to manipulate quantum systems, which has widespread applications in quantum technologies. However, for higher-dimensional complex systems, the exact CD term involving the spectral properties of the system is difficult to calculate and generally takes a complicated form, impeding its experimental realization. Recently, many approximate methods have been proposed for designing CD passages in many-body systems. In this topical review, we focus on the CD formalism and briefly introduce several experimental constructions and applications of approximate CD driving in spin-chain models with nuclear magnetic resonance (NMR) systems.

Keywords: nuclear magnetic resonance, quantum simulation, quantum state engineering

PACS: 03.67.–a, 42.50.Dv, 82.56.–b **DOI:** 10.1088/1674-1056/ad58b2

1. Introduction

Quantum information technology has ability to surpass traditional technologies because of intrinsic and intriguing features like coherence and entanglement, which involves a wide range of applications, ranging from quantum computation[1] and quantum cryptography[2] to quantum sensing.[3] Precise control of quantum systems is a fundamental prerequisite for realizing the quantum advantage. However, quantum systems inevitably suffer from noise and errors, resulting in a deviation from the ideal control, so it is a non-trivial task to implement high-quality coherent control. Despite lots of control strategies robust to environmental noise and experimental imperfections have been made,[4,5] advances in precise and fast quantum control applicable to multi-qubit systems are still widely needed.

Due to the robustness against weak variations of a quantum system, quantum adiabatic processes have been used in a variety of applications, including quantum state manipulation, quantum simulation and quantum computing.[6–11] Nevertheless, a primary constraint of this method arises from adhering to the adiabatic theorem,[12,13] which requires the system Hamiltonian to change slowly enough. Consequently, there exists a trade-off between the evolution time and decoherence processes. "Shortcut to adiabaticity" (STA) provides a method for constructing nonadiabatic schemes to accelerate the quantum adiabatic process.[14–18] Following several years of progresses, the STA-based techniques have been applied in a wide range of fields;[19–29] see Refs. [30,31] for a recent review.

As one of the most successful strategies in STA, counterdiabatic driving (CD) , also known as transitionless quantum driving, can eliminate nonadiabatic transitions by supplementing the original Hamiltonian with an auxiliary CD field,[14–16] which has been verified both experimentally and theoretically in few-level systems.[19–22,29,32,33] However, for larger systems, it is generally difficult to diagonalize the Hamiltonian in the whole Hilbert space and obtain the explicit form of the CD term. Furthermore, the CD term usually involves complex interactions in a multi-qubit system.[34–36]

To address these issues, recently various strategies have been employed to approximately construct CD driving in many-body systems with a realizable form.[36–54] With the merits of outstanding controllability, NMR has been a reliable physical platform to perform quantum simulation and quantum information processing.[55–68] In this topical review, we only focus on the CD method and introduce the recent implementations of approximate CD driving for many-body systems on NMR systems. The rest of the paper is organized as follows. In Section 2, we concisely outline the basic theory of CD driving and recent progress of approximate CD driving. Section 3 presents a quick overview of NMR quantum systems. Next, Section 4 introduces three experimental realizations of approximate CD shortcuts using NMR: (i) preparing

[†]Corresponding author. E-mail: zhouhui9240@163.com
[‡]Corresponding author. E-mail: xhpeng@ustc.edu.cn

© 2024 Chinese Physical Society and IOP Publishing Ltd

the Greenberger–Horne–Zeilinger (GHZ) states by partially suppressing the nonadiabatic transitions; (ii) realizing local CD shortcuts in a nonintegrable spin-1/2 chain based on variational approach; (iii) transferring quantum state via Floquet-engineered CD driving. Finally, a brief summary and outlook are presented in Section 5.

2. Counterdiabatic driving

The CD driving was independently proposed by Demirplak and Rice,[14,15] and by Berry.[16] There are also other basic methods of designing STA such as the invariant-based inverse engineering[17] and fast-forward scaling,[18,69] which have a close relation with the CD method. The essence of the CD driving is presented in what follows. Consider an arbitrary quantum system evolves under the time-dependent Hamiltonian

$$H_0(t)=\sum_n E_n(t)\,|n(t)\rangle\,\langle n(t)|\,, \tag{1}$$

in which $|n(t)\rangle$ denotes the n-th instantaneous eigenstate with eigenvalue $E_n(t)$. In this paper, we set $\hbar=1$ for simplicity. If the variation of $H_0(t)$ is slow enough, compared to the energy gap, such that the adiabatic condition

$$\frac{|\langle m(t)|\,\partial_t H_0\,|n(t)\rangle|}{[E_n(t)-E_m(t)]^2}\ll 1 \tag{2}$$

is satisfied for $n\neq m$, then an initial eigenstate $|n(0)\rangle$ will remain the instantaneous eigenstate during the evolution. In the adiabatic limit, the adiabatic state govern by $H_0(t)$ reads

$$|\Psi_n(t)\rangle=\mathrm{e}^{-\mathrm{i}\int_0^t \mathrm{d}t' E_n(t')-\int_0^t \mathrm{d}t'\langle n(t')|\dot{n}(t')\rangle}|n(t)\rangle, \tag{3}$$

where the first term and the second term in the exponential represent the dynamical phase and the geometric phase, respectively. If the change of the Hamiltonian is nonadiabatic, undesirable quantum transitions will take place.

Berry found that these nonadiabatic transitions can be exactly canceled by introducing an additional term to the original Hamiltonian, and thereby the speed of adiabatic evolution can be accelerated.[16] Suppose there exists a Hamiltonian $H(t)$ to be determined and the adiabatic state $|\Psi_n(t)\rangle$ is the exact solution of the Schrödinger equation

$$\mathrm{i}\frac{\mathrm{d}}{\mathrm{d}t}|\Psi_n(t)\rangle=H(t)|\Psi_n(t)\rangle. \tag{4}$$

The new Hamiltonian $H(t)$ can be easily derived as

$$H(t)=H_0(t)+H_{\mathrm{cd}}(t), \tag{5}$$

with the CD operator defined as

$$H_{\mathrm{cd}}(t)=\mathrm{i}\sum_n(1-|n(t)\rangle\langle n(t)|)|\dot{n}(t)\rangle\langle n(t)|. \tag{6}$$

If a quantum system is initialized in an eigenstate $|n(0)\rangle$ and steered by this designed Hamiltonian $H(t)$, it will track along the same eigenstate $|n(t)\rangle$. This approach enables the suppression of non-adiabatic effects and facilitates time evolution beyond the adiabatic condition.

However, for larger complex systems, it is difficult to obtain spectral properties of the system and implement highly nonlocal many-body interactions. This gives rise to the fast development of approximate CD methods, i.e., replacing the exact CD term with a simple and achievable form under experimental constraints. For instance, resorting to a set of restricted operators in auxiliary control fields, Ref. [41] obtained the optimal approximations to the CD field by minimizing a quadratic cost function, and demonstrated that the short-range few-body interactions could produce an effectively adiabatic dynamic. In the case of the infinite range Lipkin–Meshkov–Glick model, Ref. [43] provided a hybrid strategy to achieve nearly perfect CD driving across the phase transition by combining the STA and optimal control, eliminating the knowledge of the spectrum information and complicated drivings.

Considering the difficulties in diagonalizing Hamiltonian and realizing the nonlocalities of the exact CD term in complex quantum systems, the variational approach, an important advance in addressing these obstacles, was proposed to construct approximate local CD shortcuts without using spectral information.[36] The variational approach has been used to speed up the many-body systems like the p-spin model,[70,71] Lechner–Hauke–Zoller lattice gauge model,[72] Hubbard model,[73] and has great potentialities in quantum optimal control and quantum chaos.[74,75] The relationship between the variational approach and the algebraic approach has been elaborately investigated.[50] Inspired by the variational approach, employing the Lanczos algorithm to construct the CD Hamiltonian with the Krylov basis was also suggested.[76,77] Another alternative method to determine the approximate CD field is using Floquet engineering, i.e., periodic driving, which can avoid extra interactions not included in the initial control setup by fast modulating the original Hamiltonian of the system in time.[46,48,78] Recently, the strategy combining the Floquet engineering and variational method has been explored to speed up adiabatic evolution,[49] which inherits the advantages of both techniques: avoiding the need for spectral information and simplifying complex control requirements. The latest progress in studies of approximate CD driving was summarized and discussed in Ref. [79]. Readers interested in this topic can refer to it for further information.

3. Quantum simulation with NMR

Excellent reviews on NMR quantum computing can be found in Refs. [80–82]. Here we deal only with the liquid-state NMR and briefly introduce the fundamental steps of quantum

simulation with NMR, including the initial state preparation, effective Hamiltonian generation and readout. Conventionally, NMR experiments are performed in a static magnetic field B_0, where nuclei spins are thermally prepolarized (we only consider nuclear spin-1/2 in this paper), and two possible spin orientations $|\uparrow\rangle$ and $|\downarrow\rangle$ can represent two orthogonal states $|0\rangle$ and $|1\rangle$ of a quantum bit, respectively. Under the weak coupling approximation, the Hamiltonian of a liquid-state NMR system can be well described as[80]

$$H_{\rm NMR} = \sum_{i=1} \frac{\pi\omega_i}{2}\sigma_i^z + \sum_{i<j} \frac{\pi J_{ij}}{2}\sigma_i^z\sigma_j^z, \tag{7}$$

where the Larmor frequency $\omega_i = \gamma_i B_0$ with γ_i being the gyromagnetic ratio of the i-spin, and J_{ij} is the scalar coupling constant between spins i and j. Note that even for the homonuclear molecules, nuclei having the same gyromagnetic ratios, they can be well distinguished in experiments, as the nuclear shielding effect can induce frequency shifts. Figure 1 displays two frequently used NMR samples.

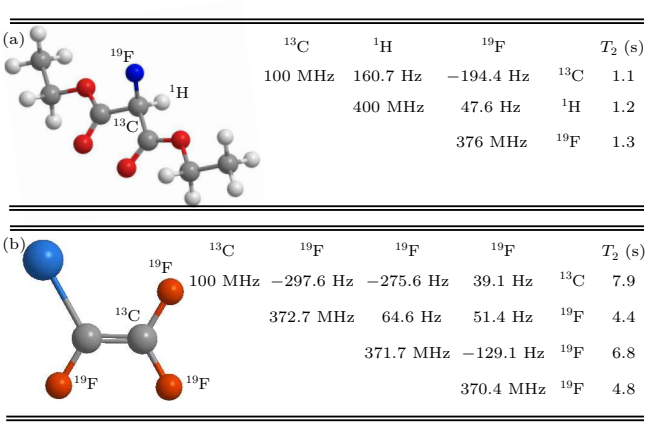


Fig. 1. Molecular structures and parameters of two representative samples: (a) diethyl-fluoromalonate and (b) iodotrifluoroethylene at room temperature on a Bruker Avance II 400 MHz spectrometer.

The first step of performing quantum computation or simulation is to initialize the quantum system into a well-defined state, generally taken as the state $|00\cdots0\rangle$. However, it is hard to generate a genuine pure state for the NMR system, on account of the highly mixed ensemble and low polarization. Instead, the standard solution in NMR is to prepare a pseudo-pure state (PPS)[83]

$$\rho_{\rm PPS} = \frac{1-\epsilon}{2^n}\boldsymbol{I} + \epsilon|00\cdots0\rangle\langle00\cdots0| \tag{8}$$

from the equilibrium state with a non-unitary process. Here $\epsilon \sim 10^{-5}$ is the polarization and the identity matrix $\boldsymbol{I}$ contributes nothing to the NMR spectra. Consequently, the dynamics of a PPS behave similarly to that of a genuine pure state. Up to now, many methods have been developed to prepare the PPS in NMR, such as temporal averaging,[84,85] line selective,[86] and so on.

Subsequently, an effective Hamiltonian can be generated by applying an external radio-frequency (RF) field

$$H_{\rm rf} = -\sum_{i}^{n} \gamma_i B_1 [\cos(\omega_{\rm rf}t + \phi)I_i^x - \sin(\omega_{\rm rf}t + \phi)I_i^y] \tag{9}$$

in the presence of the intrinsic Hamiltonian $H_{\rm NMR}$, where B_1, $\omega_{\rm rf}$, ϕ, t represent the amplitude, frequency, phase, and time length of the RF pulse, respectively. If we consider a time-dependent Hamiltonian, e.g., adiabatic or CD driving, the evolution operator can be expressed as $U(T) = \mathcal{T}(\mathrm{e}^{-\mathrm{i}\int_0^T H(t)\,\mathrm{d}t})$, where $\mathcal{T}$ denotes the time-ordering operator. For experimental implementation, the continuous passage can be discretized into M segments,[55,58] and the time interval $\delta t = T/M$ tends to zero such that the piecewise Hamiltonian in the m-th interval $H[t_m]$ can be assumed to be constant. Thus, the time evolution operator is given by $U(T) = \prod_{m=1}^{M} \mathrm{e}^{-\mathrm{i}H[t_m]\delta t}$. If $H(t)$ consists of L local components $H(t) = \sum_{k=1}^{L} H_k(t)$, the exponential $\mathrm{e}^{-\mathrm{i}H[t_m]\delta t}$ can be decomposed with the Trotter expansion[87]

$$\mathrm{e}^{-\mathrm{i}H[t_m]\delta t} = \prod_{k=1}^{L} \mathrm{e}^{-\mathrm{i}H_k[t_m]\delta t} + \mathcal{O}(\delta^2 t). \tag{10}$$

Then, each term $\mathrm{e}^{-\mathrm{i}H_k[t_m]\delta t}$ can be further implemented with the NMR pulse techniques.[80–82] By this way, the dynamics of the paradigmatic many-body systems like the Ising model, Heisenberg model and quantum Rabi model have been investigated in NMR.[55,56,58,59] Figure 2 illustrates a pulse sequence used to generate the effective CD driving in NMR experiments. The segment duration δt determines the quality of the approximation. In principle, we can resort to high-order Trotter's formula for high-accuracy dynamics. For large-size systems, multiple-pulse sequences may give rise to systematic errors and decoherence effects. To address this issue, a commonly used method is the gradient ascent pulse engineering (GRAPE) technique,[88] which can produce robust and high-fidelity coherent control in experiments.[58–61]

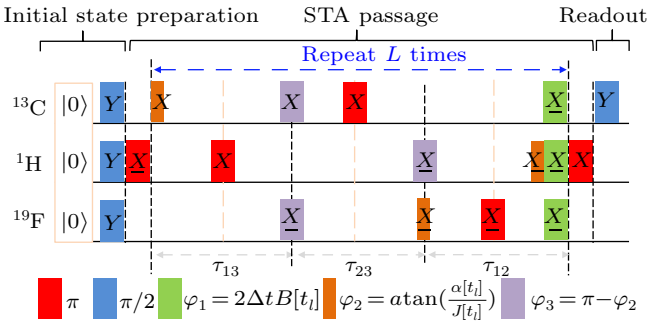


Fig. 2. Schematic pulse sequence for generating CD driving in three-qubit experiments. The color rectangles represent the hard pulses applied to individual qubits. Time durations τ_{12}, τ_{23} and τ_{13} represent free evolutions under the intrinsic Hamiltonian. This figure is adapted from Ref. [42].

As the last step, a suitable set of measurements is typically performed to extract the required information. The NMR signal is detected by the free induction decay of the transversal magnetization of spins. The errors in experiments usually

come from the imperfections of the initial state preparation, RF pulses, and inhomogeneity of magnetic fields. To get the complete form of a density matrix, one can perform quantum state tomography[89] by measuring a complete set of basis operators. Nevertheless, for large-size systems, it is challenging to perform a complete quantum state tomography due to the exponentially growing resources.

Below, we will briefly introduce several implementations and applications of approximate CD driving in spin-chain systems using NMR quantum information processor.

4. Implementations of approximate CD driving with NMR

4.1. Quantum entangled states preparation by partially suppressing the nonadiabatic transitions

Entanglement is one of the fundamental signatures of quantum physics,[90] which stays at the heart of quantum computation, quantum metrology, and so on. As a matter of concern, speeding up the generation of entangled state is highly desirable in experiment. Recently, we devised a practical protocol for preparing the GHZ state in experiments.[42] Consider a three-spin Ising model in an external magnetic field

$$H_0(t) = -B(t)\sum_{i=1}^{N}\sigma_i^x - J(t)\sum_{i=1}^{N}\sigma_i^z\sigma_{i+1}^z \tag{11}$$

with a periodic boundary condition, the ground state of this system can be adiabatically driven from the product state $[|0\rangle+|1\rangle]^{\otimes 3}$ to the GHZ state by switching from $B \gg J$ to $B \ll J$. The exact $H_{\rm cd}(t)$ involves six two-body interactions $\sum_{i\neq j}\sigma_i^z\sigma_j^y$ and six three-body interactions $\sum_{i\neq j\neq k}\sigma_i^x\sigma_j^y\sigma_k^z$. Since the inherent multi-body interaction is absent in NMR, we have to simulate it with RF pulses and two-body interactions.[55] Errors accumulated from imperfect operations will increase the difficulties in experiments.

In fact, the CD field can be simplified, if we only accelerate the adiabatic evolution for a part of the eigenstates, as shown in Refs. [39–41]. For convenience, we can represent $H_{\rm cd}(t)$ in the instantaneous eigenstate basis $\{|n(t)\rangle\}$ from the Schrödinger picture with the transformation $R=\sum_m|m(t)\rangle\langle\overline{m}|$, namely,

$$\begin{aligned} R^{\dagger}H_{\rm cd}R \;=\; & \mathrm{i}\sum_n|\overline{n}\rangle\langle\overline{n}|\langle n(t)|\dot{n}(t)\rangle \\ & +\mathrm{i}\sum_{n\neq m}|\overline{n}\rangle\langle\overline{m}|\langle n(t)|\dot{m}(t)\rangle. \end{aligned} \tag{12}$$

Here $\{|\overline{m}\rangle\}$ denotes a set of time-independent basis states satisfying the orthogonal completeness relation. The second term in Eq. (12) prevents all nonadiabatic transitions, where $\langle n(t)|\dot{m}(t)\rangle$ suppresses the nonadiabatic transition from the m-th eigenstate to the n-th eigenstate. $|\overline{n}\rangle\langle\overline{m}|$ is a matrix where all elements are zero with the exception of the m-th row and the n-th column being 1. Provided that there exists an available Hamiltonian $H_{\rm add}(t)=\sum_k\alpha_k(t)\mathcal{O}_k$ with $\alpha_k(t)$ being the time-dependent coefficient of the restricted operator $\mathcal{O}_k$. In the instantaneous eigenstate basis $\{|n(t)\rangle\}$, $H_{\rm add}(t)$ can be written as

$$R^{\dagger}H_{\rm add}R=\sum_{n,m,k}|\overline{n}\rangle\langle\overline{m}|\langle n(t)|\alpha_k(t)\mathcal{O}_k|m(t)\rangle. \tag{13}$$

If $R^{\dagger}H_{\rm add}R$ nullifies the undesired transition in Eq. (12), i.e.,

$$\sum_k\langle n(t)|\alpha_k(t)\mathcal{O}_k|m(t)\rangle=\mathrm{i}\langle n(t)|\dot{m}(t)\rangle,\quad n\neq m, \tag{14}$$

the shortcut from the m-th eigenstate to the n-th eigenstate can be constructed effectively. To ensure the feasibility of experiment, here only two-body interactions in the exact CD field,

$$\{\mathcal{O}_{k=1,\ldots,6}\}=\{\sigma_1^z\sigma_2^y,\sigma_1^y\sigma_2^z,\sigma_2^z\sigma_3^y,\sigma_2^y\sigma_3^z,\sigma_3^z\sigma_1^y,\sigma_3^y\sigma_1^z\},$$

were used to design the approximate CD passage. The additional Hamiltonian is expressed as

$$H_{\rm add}(t)=-\sum_{k=1}^{N_{\rm o}}\alpha_k(t)\mathcal{O}_k, \tag{15}$$

where $N_{\rm o}$ denotes the number of the auxiliary operators. Both $H_0(t)$ and $H_{\rm add}(t)$ commute with the operator $X=\prod_{i=1}^{3}\sigma_i^x$, so they can be simultaneously block diagonalized in the two eigenspaces $\mathcal{X}_{\pm1}$ of X with the eigenvalues ±1. Any initial state in either an orthogonal invariant subspace, driven by $H_0(t)+H_{\rm add}(t)$, would remain in the same subspace. Therefore, we only need to suppress the transitions between the ground state and other three excited states in the same subspace.

According to Eq. (14), three linear equations can enable the system to evolve exactly along the ground state and ultimately end with the GHZ state. If the number of auxiliary operators is large, the coefficient matrix of the linear equations may have a rank lower than the number of variables, potentially leading to multiple solutions. However, it is essential to ensure that the functions of coefficients are finite and smooth. In Figs. 3(a) and 3(b), we can see that some couplings near the boundary tend to be infinity, a scenario unattainable in experimental conditions, necessitating the exclusion of such solutions. A special case is obtained by imposing a constraint that $\alpha_{2,4,6}=0$, and $\alpha_{1,3,5}(t)$ can be solved exactly. As shown in Fig. 3(e), the final fidelity driven along this constructed Hamiltonian $H_0(t)+H_{\rm add}(t)$ tends to 1 quickly, which has the same precision as $H_0(t)+H_{\rm cd}(t)$. Furthermore, the number of auxiliary interactions $H_{\rm add}(t)$ is greatly reduced compared with the exact CD scheme. If the number of the operators $\{\mathcal{O}_k\}$ is limited, such as setting $\alpha_{1,3,5,6}=0$, the approximate shortcuts can still be constructed. The resulting fidelity is lower than that achieved with the exact CD protocol, but still higher than the case driven by the original Hamiltonian.

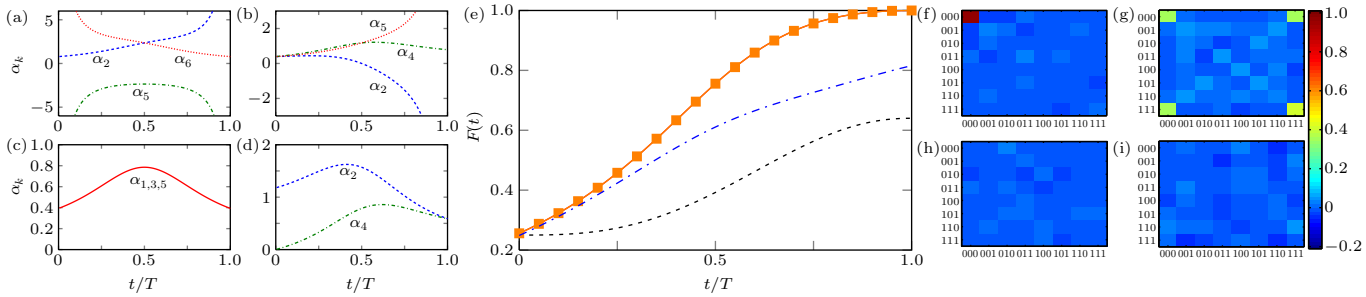


Fig. 3. (a)–(d) Time-dependent parameters $\alpha_k(t)$ on the conditions: (a) $\alpha_{1,3,4}=0$, (b) $\alpha_{1,3,6}=0$, (c) $\alpha_{2,4,6}=0$, (d) $\alpha_{1,3,5,6}=0$, respectively. (e) Quantum state fidelity of the evolved state with different protocols: no additional Hamiltonian (black dashed line), two auxiliary operators (blue dashed line), three additional operators (orange squares) and exact CD field (red solid line), respectively. (f)–(i) Experimental density matrices for the initial state $|000\rangle$ (left part), and the GHZ state (right part), where the real parts are presented in (f), (g) and imaginary parts in (h), (i). The figures are adapted from Ref. [42].

Our experiment used the diethyl-fluoromalonate dissolved in d-chloroform to simulate the three-spin chain, which consists of ^{13}C, ^{1}H, ^{19}F nuclear spins and with relevant parameters presented in Fig. 1(a). Starting from the PPS, the initial state $[|0\rangle+|1\rangle]^{\otimes 3}$ was produced by applying a y-direction $\pi/2$ pulse to three spins. To implement the approximate STA passage driven by $H(t)=H_0(t)+H_{\rm add}(t)$, the continuous evolution was discretized into many segments, in each interval the evolution operator can be approximately implemented by the Trotter's formula.[87] Finally, we performed the state tomography on the final states, and the reconstructed density matrix $\rho_{\rm exp}$ are shown in Figs. 3(g) and 3(i). The result of the experimental fidelity was about 0.94. By partially nullifying the nonadiabatic transitions, the GHZ state was successfully prepared in experiments, and this method can effectively alleviate experimental resources.

4.2. Local CD driving for a nonintegrable system based on variational approach

As described in Eq. (6), the CD term requires a spectral decomposition of the original Hamiltonian H_0. However, it is usually difficult to diagonalize the Hamiltonian in complex systems. Consider a nonintegrable spin-1/2 chain in presence of a transverse and a longitudinal magnetic field

$$H_0=J\sum_{i=1}^{N}\sigma_i^z\sigma_{i+1}^z+h_z\sum_{i=1}^{N}\sigma_i^z+h_x\sum_{i=1}^{N}\sigma_i^x. \tag{16}$$

Due to the absence of analytical solutions, obtaining the exact CD term in a larger system becomes infeasible.

Recently, the variational method was proposed to approximately obtain the best-possible CD term allowed by available resources and experimental constraints,[36] which can eliminate the need for exact diagonalization and has aroused great interest.[47,53,70,71,76,77,91] By rotating the system to the moving frame with $U[\lambda(t)]=\sum_n|n(\lambda(t))\rangle\langle\bar{n}|$, the effective Hamiltonian in this frame reads $H_0^{\rm m}=\tilde{H}_0-\dot{\lambda}\tilde{\mathcal{A}}_\lambda$, where $\tilde{H}_0=U^\dagger H_0U=\sum_n E_n(\lambda)|\bar{n}\rangle\langle\bar{n}|$ is diagonalized and $\tilde{\mathcal{A}}_\lambda=\mathrm{i}U^\dagger\partial_\lambda U$ is the adiabatic gauge potential in this moving frame. The exact CD term here can be rewritten as $H_{\rm cd}=\dot{\lambda}\mathcal{A}_\lambda$, and $\mathcal{A}_\lambda=\mathrm{i}(\partial_\lambda U)U^\dagger$ denotes the adiabatic gauge potential in the lab frame. Note that the adiabatic gauge potential $\mathcal{A}_\lambda$ satisfies the equation

$$[\mathrm{i}\partial_\lambda H_0-[\mathcal{A}_\lambda,H_0],H_0]=0. \tag{17}$$

Provided that there exists a trial adiabatic gauge potential $\mathcal{A}_\lambda^*$ in an allowed subspace, rather than in the whole Hilbert space, it has been proved that the optimal $\mathcal{A}_\lambda^*$ can be obtained by minimizing the operator distance $D^2(\mathcal{A}_\lambda^*)=\mathrm{Tr}\left[\left(G_\lambda(\mathcal{A}_\lambda)-G_\lambda(\mathcal{A}_\lambda^*)\right)^2\right]$, and here G_λ is defined by

$$G_\lambda(\mathcal{X}_\lambda)\equiv\partial_\lambda H_0+\mathrm{i}[\mathcal{X}_\lambda,H_0]. \tag{18}$$

This process is equivalent to minimizing the Hilbert–Schmidt norm of the operator $G_\lambda(\mathcal{A}_\lambda^*)$

$$\mathcal{S}(\mathcal{A}_\lambda^*)=\mathrm{Tr}\left[G_\lambda^2(\mathcal{A}_\lambda^*)\right] \tag{19}$$

with respect to $\mathcal{A}_\lambda^*$. Then, the demand for diagonalizing the Hamiltonian can be eliminated. Detailed information about the variational method can be found in Refs. [36,92]. To demonstrate the validity of this method, we experimentally constructed the local CD shortcuts for this nonintegrable spin chain.[47]

In our experiments, we utilized ^{13}C-iodotrifluoroethylene dissolved in d-chloroform as a four-qubit quantum system to realize the nonintegrable spin chain. The molecular structure and important parameters of the sample are presented in Fig. 1(b). The ground state of the Hamiltonian (16) can be created from a product state by adiabatically driving J and h_x from zero to a finite value while keeping h_z fixed. The initial state at time $t=0$ is the product state $|\Psi(0)\rangle=|1111\rangle$, which can be readily prepared from the PPS in experiments. Without loss of generality, the coupling J and transverse magnetic field h_x are changed according to the specific functions

$$h_x(t)=h_{x,f}\lambda(t),\quad J(t)=J_f\lambda(t) \tag{20}$$

with $\lambda(0)=1$ and $\lambda(T)=1$. Since this system (16) is real and satisfies time-reversal symmetry, the adiabatic gauge potential is always strictly imaginary,[36] such as $\{\sigma_i^y,\sigma_i^y\sigma_{i+1}^{z,x},\ldots\}$.

For controlling the nonlocal interactions is highly demanding in experiments, we adopted the local and simplest

adiabatic gauge potential $\mathcal{A}_\lambda^* = \beta(t)\sum_i \sigma_i^y$. Hence, by substituting it to Eq. (18), we obtained the operator $G\left(\mathcal{A}_\lambda^*\right)$, of which the Hilbert–Schmidt norm can be calculated as a quadratic form about the variable β. Minimizing the action $\mathcal{S}\left(\mathcal{A}_\lambda^*\right)$ with respect to β results in the optimal solution

$$\beta(t) = h_z\dot{h}_x/\left(2h_z^2+2h_x^2+4J^2\right). \tag{21}$$

Thus the approximate CD Hamiltonian can be given by

$$\tilde{H}(t) = H_0 + h_y\sum_{i=1}^{N}\sigma_i^y \tag{22}$$

with $h_y(t) = \dot{\lambda}(t)\cdot\beta(t)$. To evaluate the performance of the driving protocol $\tilde{H}(t)$, we also inspected the fidelities of the evolved state $|\Psi(t_m)\rangle$ with the instantaneous ground state. As shown in Fig. 4(a), the system follows the instantaneous state almost perfectly. As a comparison, only using $H_0(t)$ to drive the system under the same condition, the final fidelity dropped to only about 0.1 in experiments. It shows that this method gives an enhancement of ~ 10 times over the adiabatic evolution.

An alternative to constructing the feasible shortcuts from existing CD protocols is to perform suitable unitary transformations.[24,93,94] In experiments, we also rotated the Hamiltonian (22) by the unitary evolution operator $\overline{U}(\theta) = \prod_i e^{i\theta\sigma_i^z/2}$ with a time-dependent angle $\theta(t) = \arctan(h_y/h_x)$, and thus the auxiliary operators $\sum\sigma_i^y$ could be removed. The effective Hamiltonian turns into

$$\overline{\mathcal{H}} = \sum_{i=1}^{N}\left(h_z - \frac{1}{2}\frac{h_x\dot{h}_y - h_y\dot{h}_x}{h_x^2+h_y^2}\right)\sigma_i^z + J\sigma_i^z\sigma_{i+1}^z + \sqrt{h_x^2+h_y^2}\sigma_i^x, \tag{23}$$

which is structurally equivalent to the original one (16). It is important to highlight that this real CD protocol (23) will only drive the system along the instantaneous eigenstate of a gauge-equivalent Hamiltonian, rather than the original Hamiltonian. However, the vanishing $\dot{\lambda}(t)$ at the boundaries can lead to the coincidence of these two evolutions and generate identical results. Thus we also obtained the desired final state by utilizing $\overline{\mathcal{H}}$, but at intermediate times this system will not stay in the eigenstate of H_0. As shown in Fig. 4(a), the experimental fidelity with the real CD protocol $\overline{\mathcal{H}}$ firstly descends and then increases up to the level as the imaginary CD protocol $\tilde{H}$. Our experiments demonstrate that this variational method provides a promising approach for rapid quantum-state control in intricate and noisy quantum systems.

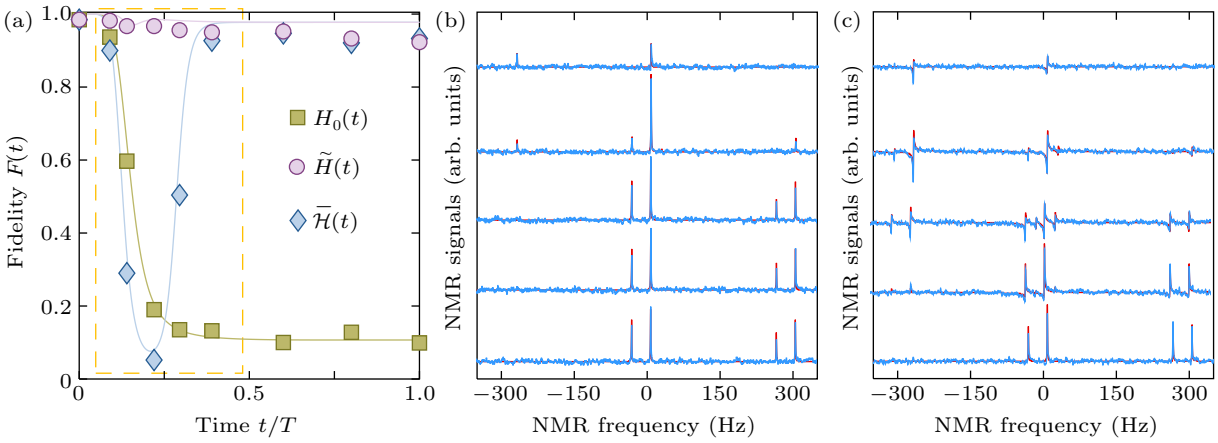


Fig. 4. (a) Experimental instantaneous fidelities with three different driving strategies: (i) the native Hamiltonian $H_0(t)$ (green squares), (ii) the image driving $\tilde{H}$ (purple circles), and (iii) the real driving $\overline{\mathcal{H}}$ (blue diamonds). (b) and (c) ^{13}C spectra of the evolved states (taking the PPS as the reference spectrum) after the $\pi/2$-readout pulse applied to the third qubit with (b) the image driving $\tilde{H}$, and (c) real driving $\overline{\mathcal{H}}$. Here we take $\lambda(t) = \sin^2\left(\frac{\pi}{2}\sin^2\left(\frac{\pi t}{2T}\right)\right)$. The figures are adapted from Ref. [47].

4.3. Quantum state transfer via Floquet-engineered CD driving

Floquet engineering provides an appealing route to quantum state manipulation, especially in complicated quantum systems. Recently, the idea of exploiting Floquet engineering, periodically modulating the parameters in H_0 to effectively mimic the dynamics of CD driving, was proposed,[46,48,49,74] which could avoid complicated interactions terms in quantum many-body systems. Inspired by these works, we designed the nonadiabatic and minimal-control quantum-state transfer (QST) in experiments. As shown in Fig. 5(a), the system involves two qubits weakly coupled to a Heisenberg chain

$$H_0(t) = J_{\rm A}(t)\boldsymbol{\sigma}_1\boldsymbol{\sigma}_2 + J_0\sum_{j=2}^{N-2}\boldsymbol{\sigma}_j\boldsymbol{\sigma}_{j+1} + J_{\rm B}(t)\boldsymbol{\sigma}_{N-1}\boldsymbol{\sigma}_N, \tag{24}$$

where the couplings satisfy the weak-couplings condition $J_{\rm A,B}(t) \ll J_0$. Our goal is to transfer an arbitrary quantum state $|\psi\rangle = a|0\rangle + b|1\rangle$ ($|a|^2+|b|^2=1$) from the qubit A to qubit B. During the process of QST, the number of excited spins is conserved. Due to the weak-couplings condition, the whole system will evolve in an invariant Zeno subspace consisting of the initial state, and thus $H_0(t)$ can be effectively simplified as

a 4×4 Hamiltonian[95]

$$H_0^{\rm e}(t)=J_{\rm A}(t)H_1^{\rm e}+J_{\rm B}(t)H_2^{\rm e}. \tag{25}$$

The parameters a and b were encoded with the eigenstates $\{|n(t)\rangle\}$ of the simplified $H_0^{\rm e}(t)$, and the perfect QST could be realized by adiabatically driving along their instantaneous eigenstate and accumulating the relative phases appropriately.

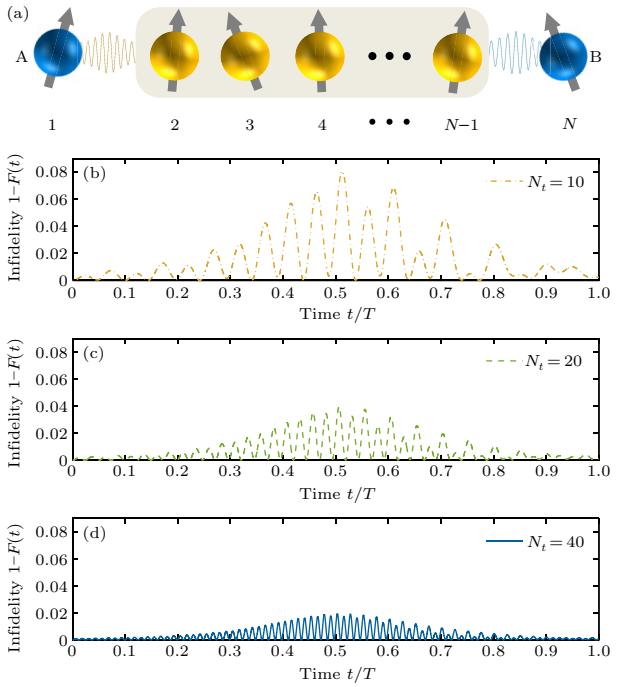


Fig. 5. (a) The schematic of QST with Floquet driving. (b)–(d) Infidelity $1-F(t)$ with the periods (b) $N_t=10$, (c) $N_t=20$ and (d) $N_t=40$.

The exact CD field $H_{\rm cd}^{\rm e}(t)$ can be calculated from $\{|n(t)\rangle\}$ in principle. However, upon returning to the full Hilbert space, this CD term involves nonlocal operators and time-dependent couplings. For example, control over a four-spin system $H_{\rm cd}^{\rm e}(t)$ requires numerous three-body and four-body interactions. Here $H_{\rm cd}^{\rm e}(t)$ is proportional to the commutator of $H_1^{\rm e}$ and $H_2^{\rm e}$, described as

$$H_{\rm cd}^{\rm e}(t)=F_{\rm cd}(t)\frac{1}{2{\rm i}}[H_1^{\rm e},H_2^{\rm e}], \tag{26}$$

with $F_{\rm cd}(t)$ being the strength of the CD field. To simulate the dynamics driven by $H_{\rm cd}^{\rm e}(t)$, the effective CD term can be constructed by $H_1^{\rm e}$ and $H_2^{\rm e}$,[48] i.e.,

$$H_{\rm Ecd}^{\rm e}(t)=c_1(t)H_1^{\rm e}+c_2(t)H_2^{\rm e}, \tag{27}$$

with the control functions $c_{1,2}(t)$ taking the form of a truncated Fourier series

$$\sum_l\left[A_l\sin(l\omega t)+B_l\cos(l\omega t)\right]. \tag{28}$$

Here ω, l, and $\{A_l,B_l\}$ denote the fundamental frequency, the truncated term, and the amplitudes, respectively.

To reproduce the CD evolution, the evolution time T will be divided into N_t periods with the duration $\tau=T/N_t$. During the n-th period, the Magnus terms for $H_{\rm cd}^{\rm e}(t)$ and $H_{\rm Ecd}^{\rm e}(t)$ can be calculated as

$$M_{\rm cd}(\tau)=-\tau F_{\rm cd}\left(t_n+\tau/2\right)\frac{[H_1^{\rm e},H_2^{\rm e}]}{2}+\mathcal{O}(\tau^3),$$
$$M_{\rm Ecd}(\tau)=-\tau\mathcal{AB}\frac{[H_1^{\rm e},H_2^{\rm e}]}{2}+\mathcal{O}(\tau^{3/2}),$$

respectively. Once the leading terms of the Magnus expansion generated by $H_{\rm Ecd}(t)$ coincide with those generated by $H_{\rm cd}^{\rm e}(t)$ up to a desired order, we can obtain the smooth control functions $\{A_l(t),B_l(t)\}$ through interpolation in different periods,[48] followed by determining the redesigned marginal couplings. This approach can significantly reduce experimental challenges by circumventing the need for controlling many-body interactions.

It should be noted that a smaller period τ signifies a higher sampling frequency of the dynamics of $H_{\rm cd}(t)$. As shown in Fig. 5, the adiabatic path can be ultimately tracked provided N_t is large enough, but this typically needs a higher oscillation frequency and stronger couplings. If the limitation of adiabaticity was somewhat relieved, the fidelity also quickly approaches 0.99 with a relatively low frequency and appropriately weak couplings in $H_{\rm Ecd}(t)$. Our experiments chose ^{13}C-iodotrifluoroethylene dissolved in d-chloroform as a four-qubit quantum system. Two sets of reconstructed density

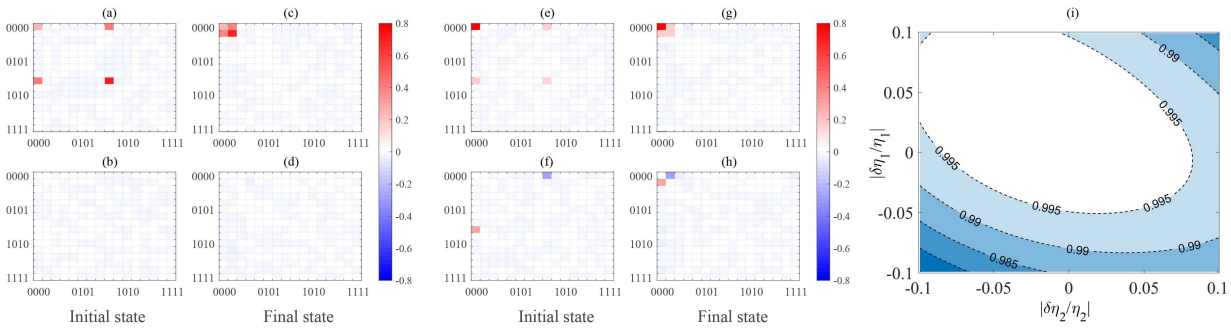


Fig. 6. (a)–(h) Experimental reconstructed density matrices of the initial states: (a), (b) $|\Psi(0)\rangle=\cos(\frac{\pi}{3})|0000\rangle+\sin(\frac{\pi}{3})|1000\rangle$, (e), (f) $|\Psi(0)\rangle=\cos(\frac{\pi}{8})|0000\rangle+{\rm e}^{{\rm i}\pi/3}\sin(\frac{\pi}{8})|1000\rangle$ and the final states (c), (d) and (g), (h). Here the upper and under figures denote the real and imaginary parts, respectively. (i) QST fidelity vs. the deviations of two designed marginal couplings $\eta_{1,2}(t)$. The figures are adapted from Ref. [51].

matrices for the initial and final states in experiments are displayed in Figs. 6(c)–6(j). To examine that the target states were sent to the end of spin chains, we obtained the reduced density matrices of the receiving spin by tracing over the sending and inner spins, of which the fidelities were all above 0.99. The results presented in Fig. 6(i) indicate that, despite marginal couplings with relative errors of 10%, the final fidelity remains above 0.97, highlighting the robustness of our scheme in the presence of errors. In a larger system, the validity and robustness of this scheme can be maintained as long as the inner coupling strength is strong enough. These experimental results confirm the feasibility of a fast QST protocol by approximatively counteracting the nonadiabatic transitions using Floquet-engineering techniques.

5. Summary and outlook

The CD driving in principle allows one to realize arbitrarily fast adiabatic processes with the help of an additional CD term, but a crucial issue emerges in many-body scenarios is that we need the spectrum properties of the system and complex resources to realize the interactions absent in the natural Hamiltonian. Here we concentrate on the constructions of the approximate CD method in spin chain systems, and provide a brief overview of its recent experimental applications using an NMR quantum processor. These experiments demonstrate the usefulness of the approximate CD technique for quantum computation and simulation via current quantum technology. It should be stressed that there still exist some questions to be further explored. For instance, the minimum required information and resource for constructing approximate CD driving in complex systems are not yet clear.

For quantum approximate optimization algorithm (QAOA), the idea of counterdiabatic QAOA (CD-QAOA)[96–101] has been explored for the Ising spin models, p-spin model, portfolio optimization and protein-folding problem. This method utilizes the additional approximate CD operators along with the Hamiltonian and mixing terms to design a better circuit ansatz. These additional free parameters enhance the degrees of freedom, facilitating access to broader parts of the Hilbert space of the Hamiltonian with a reduced circuit depth than the standard QAOA. The CD-QAOA method only requires the operator form of the CD driving, thereby avoiding the tough calculation of the time-dependent CD coefficients. The performance of CD-QAOA using higher-order CD terms was also studied.[101] It is an interesting future direction to explore the extra advantages of CD-QAOA and its challenges in experiments, such as the sensitivity to the initial parameters.

In addition to quantum computing, in the field of quantum thermodynamics, exploiting the CD driving to boost the efficiency of quantum heat engine has been proposed.[102–108] The maximal efficiency of heat engines may be achieved through the adiabatic process, but this results in the zero output power in the adiabatic limit. The tradeoff between efficiency and power is one of the focal problems in finite-time quantum thermodynamics. Reference [103] proposed to enhance the output power along with the CD driving by eliminating quantum friction and reducing the cycle time, which has been experimentally demonstrated with a trapped unitary Fermi gas as a working substance.[105] In a quantum Otto-type refrigerator[106] based on a superconducting qubit coupled to two resonant circuits, the CD technique also can counteract nonadiabatic excitations and allow a large improvement of the thermodynamic efficiency of the refrigerator. In the near future, more attention should be paid to utilizing many-body effects and the approximate, experimentally realizable CD scheme to improve the efficiency of quantum heat engine and refrigerator.

Other subjects related to the CD formalism are not included in the main text. Interested readers are advised to refer to the reviews[30,31,79] for details of this subject and other approaches to STA.

Acknowledgments

Project supported by the Innovation Program for Quantum Science and Technology (Grant No. 2021ZD0303205), the National Natural Science Foundation of China (Grant Nos. 12104282 and 12305014), the Initiative in Quantum Information Technologies of Anhui Province (Grant No. AHY050000), and the Fundamental Research Funds for the Central Universities (Grant Nos. JZ2024HGTB0253 and JZ2023HGTA0172).

References

[1] Bharti K, Cervera-Lierta A, Kyaw T H, Haug T, Alperin-Lea S, Anand A, Degroote M, Heimonen H, Kottmann J S, Menke T, Mok W K, Sim S, Kwek L C and Aspuru-Guzik A 2022 *Rev. Mod. Phys.* **94** 015004
[2] Portmann C and Renner R 2022 *Rev. Mod. Phys.* **94** 025008
[3] Degen C L, Reinhard F and Cappellaro P 2017 *Rev. Mod. Phys.* **89** 035002
[4] Suter D and Álvarez G A 2016 *Rev. Mod. Phys.* **88** 041001
[5] Koch C P, Boscain U, Calarco T, Dirr G, Filipp S, Glaser S J, Kosloff R, Montangero S, Schulte-Herbrüggen T, Sugny D and Wilhelm F K 2022 *Eur. Phys. J. Quantum Technol.* **9** 19
[6] Farhi E, Goldstone J, Gutmann S, Lapan J, Lundgren A and Preda D 2001 *Science* **292** 472
[7] Král P, Thanopulos I and Shapiro M 2007 *Rev. Mod. Phys.* **79** 53
[8] Peng X, Liao Z, Xu N, Qin G, Zhou X, Suter D and Du J 2008 *Phys. Rev. Lett.* **101** 220405
[9] Xu N, Zhu J, Lu D, Zhou X, Peng X and Du J 2012 *Phys. Rev. Lett.* **108** 130501
[10] Cirac J I and Zoller P 2012 *Nat. Phys.* **8** 264
[11] Albash T and Lidar D A 2018 *Rev. Mod. Phys.* **90** 015002
[12] Born M and Fock V 1928 *Z. Phys.* **51** 165
[13] Kato T 1950 *J. Phys. Soc. Jpn.* **5** 435
[14] Demirplak M and Rice S A 2003 *J. Phys. Chem. A* **107** 9937
[15] Demirplak M and Rice S A 2005 *J. Phys. Chem. B* **109** 6838
[16] Berry M V 2009 *J. Phys. A* **42** 365303
[17] Chen X, Ruschhaupt A, Schmidt S, del Campo A, Guéry-Odelin D and Muga J G 2010 *Phys. Rev. Lett.* **104** 063002
[18] Masuda S and Nakamura K 2010 *Proc. R. Soc. A* **466** 1135

[19] Zhang J, Shim J H, Niemeyer I, Taniguchi T, Teraji T, Abe H, Onoda S, Yamamoto T, Ohshima T, Isoya J and Suter D 2013 *Phys. Rev. Lett.* **110** 240501
[20] Yan T, Liu B J, Xu K, Song C, Liu S, Zhang Z, Deng H, Yan Z, Rong H, Huang K, Yung M H, Chen Y and Yu D 2019 *Phys. Rev. Lett.* **122** 080501
[21] Du Y X, Liang Z T, Li Y C, Yue X X, Lv Q X, Huang W, Chen X, Yan H and Zhu S L 2016 *Nat. Commun.* **7** 12479
[22] An S, Lv D, del Campo A and Kim K 2016 *Nat. Commun.* **7** 12999
[23] Okuyama M and Takahashi K 2016 *Phys. Rev. Lett.* **117** 070401
[24] Baksic A, Ribeiro H and Clerk A A 2016 *Phys. Rev. Lett.* **116** 230503
[25] Campbell S and Deffner S 2017 *Phys. Rev. Lett.* **118** 100601
[26] Funo K, Zhang J N, Chatou C, Kim K, Ueda M and del Campo A 2017 *Phys. Rev. Lett.* **118** 100602
[27] Kleissler F, Lazariev A and Arroyo-Camejo S 2018 *npj Quantum. Inf.* **4** 49
[28] Vepsäläinen A, Danilin S and Paraoanu G S 2019 *Sci. Adv.* **5** eaau5999
[29] Zhou B B, Baksic A, Ribeiro H, Yale C G, Heremans F J, Jerger P C, Auer A, Burkard G, Clerk A A and Awschalom D D 2017 *Nat. Phys.* **13** 330
[30] Guéry-Odelin D, Ruschhaupt A, Kiely A, Torrontegui E, Martínez-Garaot S and Muga J G 2019 *Rev. Mod. Phys.* **91** 045001
[31] del Campo A and Kim K 2019 *New J. Phys.* **21** 050201
[32] Chen X, Lizuain I, Ruschhaupt A, Guéry-Odelin D and Muga J G 2010 *Phys. Rev. Lett.* **105** 123003
[33] Smith A, Lu Y, An S, Zhang X, Zhang J N, Gong Z, Quan H T, Jarzynski C and Kim K 2018 *New J. Phys.* **20** 013008
[34] del Campo A, Rams M M and Zurek W H 2012 *Phys. Rev. Lett.* **109** 115703
[35] Takahashi K 2013 *Phys. Rev. E* **87** 062117
[36] Sels D and Polkovnikov A 2017 *Proc. Natl. Acad. Sci. USA* **114** E3909
[37] del Campo A 2013 *Phys. Rev. Lett.* **111** 100502
[38] Ibáñez S, Chen X and Muga J G 2013 *Phys. Rev. A* **87** 043402
[39] Opatrný T and Mølmer K 2014 *New J. Phys.* **16** 015025
[40] Chen Y H, Xia Y, Wu Q C, Huang B H and Song J 2016 *Phys. Rev. A* **93** 052109
[41] Saberi H, Opatrný T c v, Mølmer K and del Campo A 2014 *Phys. Rev. A* **90** 060301
[42] Ji Y, Bian J, Chen X, Li J, Nie X, Zhou H and Peng X 2019 *Phys. Rev. A* **99** 032323
[43] Campbell S, De Chiara G, Paternostro M, Palma G M and Fazio R 2015 *Phys. Rev. Lett.* **114** 177206
[44] Kyaw T H and Kwek L C 2018 *New J. Phys.* **20** 045007
[45] Zhou H, Dai X, Geng J, Jin F and Ji Y 2024 *Phys. Lett. B* **852** 138632
[46] Boyers E, Pandey M, Campbell D K, Polkovnikov A, Sels D and Sushkov A O 2019 *Phys. Rev. A* **100** 012341
[47] Zhou H, Ji Y, Nie X, Yang X, Chen X, Bian J and Peng X 2020 *Phys. Rev. Appl.* **13** 044059
[48] Petiziol F, Dive B, Mintert F and Wimberger S 2018 *Phys. Rev. A* **98** 043436
[49] Claeys P W, Pandey M, Sels D and Polkovnikov A 2019 *Phys. Rev. Lett.* **123** 090602
[50] Hatomura T and Takahashi K 2021 *Phys. Rev. A* **103** 012220
[51] Zhou H, Chen X, Nie X, Bian J, Ji Y, Li Z and Peng X 2019 *Sci. Bull.* **64** 888
[52] Mbeng G B and Lechner W 2022 arXiv:2207.03553 [quant-ph]
[53] Ji Y, Zhou F, Chen X, Liu R, Li Z, Zhou H and Peng X 2022 *Phys. Rev. A* **105** 052422
[54] Ji Y, Wu Z, Liu R, Li Y, Jin F, Zhou H and Peng X 2024 *New J. Phys.* **26** 013041
[55] Peng X, Zhang J, Du J and Suter D 2009 *Phys. Rev. Lett.* **103** 140501
[56] Du J, Xu N, Peng X, Wang P, Wu S and Lu D 2010 *Phys. Rev. Lett.* **104** 030502
[57] Feng G, Xu G and Long G 2013 *Phys. Rev. Lett.* **110** 190501
[58] Li Z, Zhou H, Ju C, Chen H, Zheng W, Lu D, Rong X, Duan C, Peng X and Du J 2014 *Phys. Rev. Lett.* **112** 220501
[59] Chen X, Wu Z, Jiang M, Lü X Y, Peng X and Du J 2021 *Nat. Commun.* **12** 6281
[60] Nie X, Wei B B, Chen X, Zhang Z, Zhao X, Qiu C, Tian Y, Ji Y, Xin T, Lu D and Li J 2020 *Phys. Rev. Lett.* **124** 250601
[61] Xin T, Che L, Xi C, Singh A, Nie X, Li J, Dong Y and Lu D 2021 *Phys. Rev. Lett.* **126** 110502
[62] Long X, He W T, Zhang N N, Tang K, Lin Z, Liu H, Nie X, Feng G, Li J, Xin T, Ai Q and Lu D 2022 *Phys. Rev. Lett.* **129** 070502
[63] Li J, Luo Z, Xin T, Wang H, Kribs D, Lu D, Zeng B and Laflamme R 2019 *Phys. Rev. Lett.* **123** 030502
[64] Li K, Wan Y, Hung L Y, Lan T, Long G, Lu D, Zeng B and Laflamme R 2017 *Phys. Rev. Lett.* **118** 080502
[65] Peng X, Zhou H, Wei B B, Cui J, Du J and Liu R B 2015 *Phys. Rev. Lett.* **114** 010601
[66] Luo Z, Li J, Li Z, Hung L Y, Wan Y, Peng X and Du J 2018 *Nat. Phys.* **14** 160
[67] Liu R, Chen Y, Jiang M, Yang X, Wu Z, Li Y, Yuan H, Peng X and Du J 2021 *npj Quantum Information* **7** 170
[68] Wu Z, Wang P, Wang T, Li Y, Liu R, Chen Y, Peng X and Liu R B 2024 *Phys. Rev. Lett.* **132** 200802
[69] Torrontegui E, Martínez-Garaot S, Ruschhaupt A and Muga J G 2012 *Phys. Rev. A* **86** 013601
[70] Passarelli G, Cataudella V, Fazio R and Lucignano P 2020 *Phys. Rev. Res.* **2** 013283
[71] Prielinger L, Hartmann A, Yamashiro Y, Nishimura K, Lechner W and Nishimori H 2021 *Phys. Rev. Res.* **3** 013227
[72] Hartmann A and Lechner W 2019 *New. J. Phys.* **21** 043025
[73] Xie Q, Seki K and Yunoki S 2022 *Phys. Rev. B* **106** 155153
[74] Schindler P M and Bukov M 2024 arXiv:2310.02728 [quant-ph]
[75] Orlov P, Tiutiakina A, Sharipov R, Petrova E, Gritsev V and Kurlov D V 2023 *Phys. Rev. B* **107** 184312
[76] Bhattacharjee B 2023 arXiv:2302.07228 [quant-ph]
[77] Takahashi K and del Campo A 2024 *Phys. Rev. X* **14** 011032
[78] Petiziol F, Dive B, Carretta S, Mannella R, Mintert F and Wimberger S 2019 *Phys. Rev. A* **99** 042315
[79] Hatomura T 2024 *J. Phys. B: At. Mol. Opt. Phys.* **57** 102001
[80] Vandersypen L M K and Chuang I L 2005 *Rev. Mod. Phys.* **76** 1037
[81] Peng X H and Suter D 2010 *Front. Phys. China* **5** 1
[82] Jones J A 2024 *Prog. Nucl. Magn. Reson. Spectrosc.* **140** 49
[83] Gershenfeld N A and Chuang I L 1997 *Science* **275** 350
[84] Knill E, Chuang I and Laflamme R 1998 *Phys. Rev. A* **57** 3348
[85] Vandersypen L M K, Steffen M, Breyta G, Yannoni C S, Cleve R and Chuang I L 2000 *Phys. Rev. Lett.* **85** 5452
[86] Peng X, Zhu X, Fang X, Feng M, Gao K, Yang X and Liu M 2001 *Chem. Phys. Lett.* **340** 509
[87] Suzuki M 1993 *Proc. Jpn. Acad. Ser. B* **69** 161
[88] Khaneja N, Reiss T, Kehlet C, Schulte-Herbruggen T and Glaser S 2005 *J. Magn. Reson.* **172** 296
[89] Lee J S 2002 *Phys. Lett. A* **305** 349
[90] Horodecki R, Horodecki P, Horodecki M and Horodecki K 2009 *Rev. Mod. Phys.* **81** 865
[91] Čepaitė I, Polkovnikov A, Daley A J and Duncan C W 2023 *PRX Quantum* **4** 010312
[92] Kolodrubetz M, Sels D, Mehta P and Polkovnikov A 2017 *Phys. Rep.* **697** 1
[93] Ibáñez S, Chen X, Torrontegui E, Muga J G and Ruschhaupt A 2012 *Phys. Rev. Lett.* **109** 100403
[94] Kang Y H, Chen Y H, Shi Z C, Huang B H, Song J and Xia Y 2018 *Phys. Rev. A* **97** 033407
[95] Huang B H, Kang Y H, Chen Y H, Shi Z C, Song J and Xia Y 2018 *Phys. Rev. A* **97** 012333
[96] Chandarana P, Hegade N N, Paul K, Albarrán-Arriagada F, Solano E, del Campo A and Chen X 2022 *Phys. Rev. Res.* **4** 013141
[97] Wurtz J and Love P J 2022 *Quantum* **6** 635
[98] Chandarana P, Hegade N N, Montalban I, Solano E and Chen X 2023 *Phys. Rev. Appl.* **20** 014024
[99] Guan H, Zhou F, Albarrán-Arriagada F, Chen X, Solano E, Hegade N N and Huang H L 2023 arXiv:2311.06682 [quant-ph]
[100] Chandarana P, Paul K, de Andoin M G, Ban Y, Sanz M and Chen X 2023 arXiv:2307.14853 [quant-ph]
[101] Vizzuso M, Passarelli G, Cantele G and Lucignano P 2024 *New J. Phys.* **26** 013002
[102] del Campo A, Goold J and Paternostro M 2014 *Sci. Rep.* **4** 6208
[103] Beau M, Jaramillo J and del Campo A 2016 *Entropy* **18** 168
[104] Cakmak B and Mustecaplioglu O E 2019 *Phys. Rev. E* **99** 032108
[105] Deng S, Chenu A, Diao P, Li F, Yu S, Coulamy I, del Campo A and Wu H 2018 *Sci. Adv.* **4** eaar5909
[106] Funo K, Lambert N, Karimi B, Pekola J P, Masuyama Y and Nori F 2019 *Phys. Rev. B* **100** 035407
[107] Hartmann A, Mukherjee V, Niedenzu W and Lechner W 2020 *Phys. Rev. Res.* **2** 023145
[108] Williamson L A and Davis M J 2024 *Phys. Rev. B* **109** 024310